(15) B. J. Brisdon and D. A. Edwards, *Inorg. Nucl. Chem. Lett.*, **10**, 301 (1974).
(16) "International Tables for X-Ray Crystallography", Vol. IV, Kynoch Press, Birmingham, England, 1974, Tables 2.2A and 2.3.1.
(17) A. C. Larson in "Crystallographic Computing", F. R. Ahmed, Ed., Munksgaard, Copenhagen, 1970, p 291.
(18) T. Inazu, H. Okawa, and T. Yoshino, *Bull. Chem. Soc. Jpn.*, **42**, 2291 (1969).
(19) K. Kasuga, T. Hon, and Y. Yamamoto, *Bull. Chem. Soc. Jpn.*, **47**, 1026 (1974).
(20) J. A. Bertrand and R. I. Kaplan, *Inorg. Chem.*, **4**, 1657 (1965).
(21) C. H. S. Wu, G. R. Rossman, H. B. Gray, G. S. Hammond, and H. S. Schugar, *Inorg. Chem.*, **11**, 990 (1972).
(22) W. S. Geary, *Coord. Chem. Rev.*, 7, 781 (1971).
(23) J. F. Coetzee and G. R. Cunningham, *J. Am. Chem. Soc.*, **87**, 2529 (1965); M. S. Elder, G. M. Prinz, P. Thornton, and D. H. Busch, *Inorg. Chem.*, **7**, 2426 (1968); A. Davison, D. V. Howe, and E. J. Shawl, *ibid.*, **6**, 458 (1967); F. A. Cotton, W. R. Robinson, R. A. Walton, and R. Whyman, *ibid.*, **6**, 929 (1967).
(24) P. W. Smith and A. G. Wedd, *J. Chem. Soc. A*, 2447 (1970); I. E. Grey and P. W. Smith, *Aust. J. Chem.*, **22**, 121 (1969).
(25) E. M. Sung and M. D. Harmony, *J. Am. Chem. Soc.*, **99**, 5603 (1977).
(26) The uncertainties quoted as ± are estimated standard deviations of the sample of values measured for each structure.
(27) G. Bunzey and J. H. Enemark, *Inorg. Chem.*, **17**, 682 (1978).
(28) C. D. Garner, L. H. Hill, F. E. Mabbs, D. L. McFadden, and A. T. McPhail, *J. Chem. Soc., Dalton Trans.*, 853 (1977).
(29) R. Mattes, D. Altmeppen, and M. Fetzer, *Z. Naturforsch.*, **316**, 1356 (1976).
(30) I. G. Dance and J. C. Calabrese, *J. Chem. Soc., Chem. Commun.*, 762 (1975).
(31) I. G. Dance, *J. Chem. Soc., Chem. Commun.*, 103 (1976); *Aust. J. Chem.*, in press.
(32) The anion $[Mo_2O_4(NCS)_4(CH_3CO_2)]^{3-}$ contains[33] an $Mo_2O_4$ unit supplemented by a bridging bidentate acetate ligand, whose bite allows it to supply a ligand atom at positions trans to both terminal oxo groups, completing six-coordination around each molybdenum. This and similar species[34] are closely related to the $Mo_2O_2X_2$-based structures (Figure 1c) and not relevant to the triply bridged species discussed here.
(33) T. Glowiak, M. Sabat, H. Sabat, and M. F. Rudolf, *J. Chem. Soc., Chem. Commun.*, 712 (1975).
(34) B. Jezowska-Trzebiatowska, M. F. Rudolf, L. Natkamic, and H. Sabat, *Inorg. Chem.*, **13**, 617 (1974); T. Glowiak, M. F. Rudolf, M. Sabat, and B. Jezowska-Trzebiatowska, *J. Less-Common Met.*, **54**, 35 (1977).
(35) However, the compound $[Mo_2O_3Cl_2L_2]$ (LH = 8-aminoquinoline) appears to contain a triple bridge consisting of an oxo and two (inequivalent) NH groups from the amido functions of the quinolate ligand: I. W. Boyd and A. G. Wedd, unpublished results.
(36) I. G. Dance, unpublished results.

Contribution from the School of Chemical Sciences, University of Illinois, Urbana, Illinois 61801

# Complexes as Ligands. 2. Structural, Spectral, and Magnetic Properties of the Bimetallomer Formed from *N,N'*-Ethylenebis(salicylideniminato)copper(II) and Bis(hexafluoroacetylacetonato)copper(II)

KENNETH A. LESLIE, RUSSELL S. DRAGO,* GALEN D. STUCKY,* DAVID J. KITKO, and JOHN A. BREESE

*Received October 6, 1978*

As a continuation of our studies of complexes as ligands, we have investigated the bimetallomer Cu(salen)Cu(hfac)$_2$, which is the adduct formed by the reaction of the Lewis base *N,N'*-ethylenebis(salicylideniminato)copper(II) with the Lewis acid bis(hexafluoroacetylacetonato)copper(II). Since this bimetallomer contains two different copper(II) environments (six-coordinate and four-coordinate), magnetic susceptibility and EPR spectral studies were undertaken in order to characterize the system. Variable-temperature magnetic susceptibility measurements indicate an antiferromagnetic exchange interaction with a coupling constant, $J$, between the copper(II) centers of $-20.4$ cm$^{-1}$. In order to explain the relatively small value of $J$ when compared to that of symmetric copper(II) bimetallomers, a single-crystal X-ray diffraction study was carried out. The compound crystallizes in the triclinic space group $P\bar{1}$ with four molecules in the unit cell. The reduced cell parameters are $a$ = 17.03 (4) Å, $b$ = 19.11 (4) Å, $c$ = 9.89 (2) Å, $\alpha$ = 96.58 (11)°, $\beta$ = 100.10 (16)°, and $\gamma$ = 107.70 (13)°. The structure was refined by full-matrix least-squares methods to a weighted $R$ factor of 0.074 for data with $F_o \geq 3\sigma_F$. The structural results indicate that the reduced value of $J$ is due to the low symmetry of the bridge area which allows for only one phenolic oxygen to participate in the superexchange pathway.

## Introduction

An earlier X-ray crystallographic investigation indicated[1] that the complexes $Cu^{II}$salen and $Co^{II}(hfac)_2$ reacted to form a bimetallomer in which the oxygen donor atom of salen was simultaneously coordinated to copper and cobalt. It was also shown that the following reaction, leading to this product, was very rapid in dilute dichloromethane solution:

$$Co(salen) + Cu(hfac)_2 \rightarrow Cu(salen)Co(hfac)_2$$

The rapid metal swapping of a tetradentate chelate in $CH_2Cl_2$ was very surprising, and a kinetic study was undertaken to ascertain the mechanism.[2]

In the course of these studies, the complex Cu(salen)Cu(hfac)$_2$ was prepared. Since relatively few[3,4] copper(II) bimetallomers have been investigated in which the environment around the interacting coppers is different, magnetic investigations were undertaken. The difference in the results obtained for the complex from those expected[5,6] from theory and experiment for a symmetric bimetallomer (with a bridge angle corresponding to that found in the copper–cobalt adduct) led us to pursue a full structural characterization of the Cu(salen)Cu(hfac)$_2$ complex.

## Experimental Section

Cu(salen)Cu(hfac)$_2$ was prepared as previously reported.[2] Anal. Calcd for $Cu_2C_{26}H_{16}N_2O_6F_{12}$: Cu, 15.74; C, 38.67; H, 2.00; N, 3.47; F, 28.23. Found: Cu, 15.82; C, 39.54; H, 2.00; N, 3.44; F, 28.22.

Ni(salen)Zn(hfac)$_2$ was prepared by the procedure described for Cu(salen)Co(hfac)$_2$.[1] Ni(salen) (0.98 g, 3 mmol) and Zn(hfac)$_2$·2H$_2$O (1.55 g, 3 mmol) were employed as starting materials, having been prepared from nickel acetate and zinc acetate, respectively; yield 2.0 g (79%). Anal. Calcd for $ZnNiC_{26}H_{16}N_2O_6F_{12}$: Zn, 8.13; Ni, 7.30; C, 38.82; H, 2.00; N, 3.48. Found: Zn, 8.05; Ni, 7.23; C, 38.45; H, 2.01; N, 3.41.

**Physical Measurements.** Variable-temperature (4.2–270 K) magnetic susceptibility measurements were carried out with a Princeton Applied Research Model 150A vibrating-sample magnetometer calibrated with $CuSO_4·5H_2O$.[7] All molar susceptibilities were corrected for diamagnetic contributions by using Pascal's constants.[8] A least-squares fitting of the data was carried out with the function minimization program STEPT.[9]

Electron spin resonance spectra were collected on a Varian Model E-9 spectrometer operating at ca. 9.1 GHz (X-band) and equipped

0020-1669/79/1318-1885$01.00/0 

with a Hewlett-Packard frequency counter. The field was calibrated with a Varian weak pitch sample with $g = 2.0070$.[10] Temperature control was maintained in the range 6–50 K through the use of an Air Products Heli-tran cryogenic system. A Varian temperature controller was used to control the temperature in the range between liquid nitrogen temperature and room temperature. Samples were run as powders and as $1 \times 10^{-3}$ M frozen solutions in a 3:2 (v/v) mixture of deoxygenated toluene and $CH_2Cl_2$.

**X-ray Data.** Very dark copper-colored platelets of Cu(salen)-$Cu(hfac)_2$ were grown by slow evaporation of a saturated methylene chloride colution. A crystal (dimensions 0.25 mm × 0.48 mm × 0.12 mm) was mounted on a glass fiber for preliminary Weissenberg photographs, which revealed that the crystal was triclinic (no systematic absences) and belonged to either space group $P1$ or $P\bar{1}$.

The crystal was transferred to a Picker four-circle diffractometer, and lattice parameters were obtained by a least-squares refinement of 28 hand-centered reflections. The true reduced cell parameters were then obtained by using the program TRACER,[11] which converted the original cell parameters into those giving the smallest cell (i.e., the cell whose axes are the three shortest noncoplanar lattice translations). The final values obtained were $a = 17.03$ (4) Å, $b = 19.11$ (4) Å, $c = 9.89$ (2) Å, $\alpha = 96.58$ (11)°, $\beta = 100.10$ (16)°, $\gamma = 107.70$ (13)°, and $V = 2970$ Å$^3$. Flotation in bromoform and hexane gave a measured density of 1.79 (2) g/cm$^3$, which agrees with the value 1.81 g/cm$^3$ calculated on the assumption that $Z = 4$. This gives a value of $F(000) = 1600$. $\omega$ scans of several low-angle reflections showed widths at half-peak height of approximately 0.10°.

Intensity data were measured on a fully automatic Picker four-circle diffractometer with Mo K$\alpha$ radiation (0.710 69 Å) from a pyrolytic graphite monochromator. A $\theta$–$2\theta$ scan technique was used with a scan width of 2.0°, a scan rate of 2°/min, and a takeoff angle of 1.7°. Background counts were measured for 10 s at each end of the scanned range. Two standards were measured every 50 reflections to check for crystal and counter stability. The crystal was recentered and data recollected whenever the standards changed more than 5%. A half sphere of data ($-h,\pm k,\pm l$) was collected over the range $4° \leq 2\theta \leq 55°$; 9154 independent reflections were obtained of which 4663 were considered observed by the criterion $I_{obsd} \geq \sigma_c(I)$. Here

$$\sigma_c(I) = [T_c + (t_c/t_b)^2(B1 + B2)]^{1/2}$$

where $T_c$ is total counts, $t_c/t_b$ is the ratio of the time counting peak intensity to that counting backgrounds, and B1 and B2 are the background counts. Lorentz–polarization corrections and calculations of the observed structure factor amplitudes from the raw data were carried out with the program VANDY1.[12] The Lorentz–polarization factor is given by $Lp = (\cos^2 2\theta + \cos^2 2\theta_M)/[(\sin 2\theta)(1 + \cos^2 2\theta_M)]$ where $2\theta_M = 11.944°$. The structure factor amplitudes were assigned standard deviations according to

$$\sigma_F = \frac{[T_c + (t_c/t_b)^2(B1 + B2) + (0.03I_{rel})^2]^{1/2}}{2(Lp)^{1/2}I_{rel}^{1/2}}$$

where $I_{rel} = T_c - (t_c/t_b)(B1 + B2)$.

Absorption corrections were made ($\mu = 16.04$ cm$^{-1}$) with the program ORABS II.[13] Transmission factors ranged from 0.459 to 0.732.

**Structure Determination and Refinement.** The noncentrosymmetric space group was initially ruled out on the basis of an $N(z)$ test[14] which showed that the distribution of intensities closely matched the theoretical centrosymmetric distribution. By use of $P\bar{1}$ as the space group, the structure was solved by standard heavy-atom methods.[15] No attempt was made to locate hydrogen atoms (vide infra). Initial refinement was done with a Xerox Σ-5 computer and final refinement made use of the University of Illinois CDC CYBER 175 computer.

Neutral atomic scattering factors for all atoms were obtained from the compilations of Cromer and Waber,[16] and the anomalous dispersion terms for copper were taken from the compilation of Cromer and Liberman.[17] The structure was refined by full-matrix, least-squares techniques, minimizing the function $\sum w(|F_o| - |F_c|)^2$ with the weights being set equal to $1/\sigma_F^2$. The agreement indices are defined as $R = \sum(|F_o| - |F_c|)/\sum|F_o|$ and $R_w = (\sum w(|F_o| - (|F_c|)^2/\sum wF_o^2)^{1/2}$. The "goodness of fit" or standard deviation of an observation of unit weight is defined by GOF = $[\sum w(|F_o| - |F_c|)^2/(n - p)]^{1/2}$ where $n$ is the number of reflections used in refinement and $p$ is the number of parameters varied.

Two of the copper atoms were located from a three-dimensional Patterson map. After initial difficulty, the four copper atoms and the six oxygen atoms were positioned correctly. The remaining atoms were located in seven successive Fourier maps. Refinement of positional parameters for all 96 atoms and isotropic thermal parameters for all atoms except fluorine atoms resulted in $R_w = 0.134$. A difference Fourier map was used to reposition the fluorine atoms. Computer storage limitations required that the structure be refined in three sections. The $CF_3$ groups were refined in one section with the remaining atoms of molecule "A" and molecule "B" (see Discussion) being refined in sections two and three. Isotropic thermal parameters for the fluorine atoms were then allowed to vary, and anisotropic thermal parameters were introduced for all non-$CF_3$ group atoms. Two cycles of refinement for each of the three sections reduced $R_w$ to 0.113.

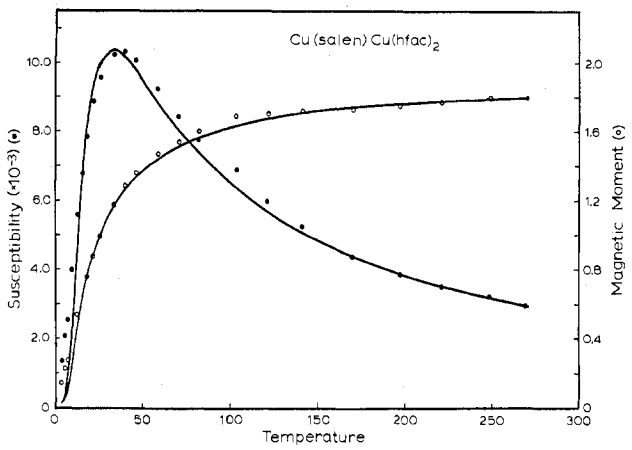


**Figure 1.** Plot of magnetic susceptibility (●) and magnetic moment (○) per Cu atom vs. temperature. Smooth curves represent the best-fit calculated curves and ● and ○ the experimental points.

A difference Fourier map showed extensive disorder among the $CF_3$ groups, the worst being the $CF_3$ groups containing (F4, F5, F6), (F4B, F5B, F6B), and (F7B, F8B, F9B). The map also suggested that the best model to fit these three groups was one containing two $CF_3$ orientations which had unequal occupancy. Subsequent least-squares refinement proved this to be an insufficient model as the occupancy factors of some of the fluorine atom positions consistently went negative. Due to time limitations and the prohibitive cost involved (a typical full-matrix least-squares cycle took 900 s and cost $600 on the CYBER), the disorder problem was not pursued further. The three most populated fluorine atom positions for each $CF_3$ group as determined from a difference Fourier map were chosen, and subsequent refinements of positional and anisotropic thermal parameters for all 96 atoms yielded a final weighted $R$ factor for all observed data of 0.081 with a GOF = 1.33. Refinement based on the observed data ($F_o \geq 3\sigma_F$) resulted in convergence with agreement factors $R = 0.117$ and $R_w = 0.074$. The GOF was 1.55. Owing to the large number of atoms in the unit cell (96) and the fact that one-third of the nonhydrogen atoms in the asymmetric unit consist of $CF_3$ groups with a high degree of thermal motion, hydrogen atoms were not included in the refinement. A final difference Fourier map showed regions of positive electron density near the $CF_3$ groups of 1.2 e/Å$^3$. The difference map also did not indicate the presence of any methylene chloride molecules.

## Results and Discussion

**Susceptibility Studies.** The room-temperature susceptibility of Cu(salen)$Cu(hfac)_2$ as determined by the Evans method indicated the absence of any substantial antiferromagnetic exchange interaction in the system. This result stands in contrast to the relatively large antiferromagnetic exchange interactions found[4] in the Cu(SB)·$CuX_2$ system (where SB stands for Schiff base and X is a halogen). Variable-temperature magnetic susceptibility determinations were carried out and the results are graphically displayed in Figure 1 and presented in tabular form in the supplementary material. A maximum is seen in the plot of susceptibility vs. temperature at approximately 37 K, indicating a small antiferromagnetic exchange interaction. The magnetic susceptibility vs. tem-

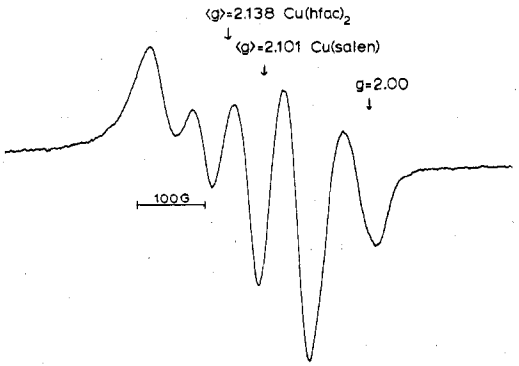


**Figure 2.** Isotropic X-band EPR spectrum for Cu(salen)Cu(hfac)$_2$ in 3/2 (v/v) toluene/$CH_2Cl_2$.

perature data were least-squares fit to the Bleaney–Bowers equation for symmetric pairwise exchange

$$\chi_M = \frac{Ng^2\beta^2}{3k(T-\Theta)}(1 + \tfrac{1}{3}\exp(-2J/kT))^{-1} + N\alpha$$

by using STEPT. In this equation, $\chi_M$ represents the molar susceptibility per bimetallomer, and $N$, $g$, $\beta$, $k$, and $T$ have their usual meaning. $N\alpha$ represents a temperature-independent paramagnetism and was taken to be $120 \times 10^{-6}$ cgsu/mol. $\Theta$ is the Curie–Weiss constant and is employed to gauge intermolecular interactions. $J$ is the exchange parameter.

The $g$ value of 2.16, taken from the ESR spectrum of a powdered sample at ca. 80 K (vide infra), was fixed in these calculations. The best fit is represented by the solid lines in Figure 1, and the best fit parameters were $J = -12.7$ cm$^{-1}$ and $\Theta = -24$ K with a standard error = 0.054. The rather large negative $\Theta$ required for the fit was considered unrealistic, and the calculations were repeated with $\Theta$ fixed at zero. The best fit under this restriction which allows only the variation of one parameter was obtained with $J = -20.4$ cm$^{-1}$ and a standard error of 0.092.

The lack of a truly good fit for the temperature dependence of the susceptibility by using the Bleaney–Bowers equation is not unexpected. This equation was derived for the treatment of symmetric, coupled copper(II) pairs. In Cu(salen)Cu(hfac)$_2$ the Cu(II) ions are in drastically different environments, and the presence of antisymmetric- and anisotropic-exchange interactions are expected. The improved fit obtained by allowing $\Theta$ to vary is expected, but its large negative value is unrealistic. It is generally included to gauge intermolecular interactions which are expected to be small in this complex. Therefore, the inclusion of $\Theta$ as a variable merely improves the fit without improving our understanding of the situation.

The value of $J = -20.4$ cm$^{-1}$ is interesting in light of the correlations made by Hatfield. While his correlation of the Cu–O–Cu bridge angle with the magnitude of $J$ cannot be directly applied to bimetallomers consisting of two different copper environments, systems in which $J$ deviates from that expected for the symmetrical bimetallomers provide the most interesting systems for obtaining fundamental information on the factors influencing exchange. If the Cu–O–Cu bridge angles in our system were the same as those in the Cu–O–Co system, the value of $J$ obtained (−20.4 cm$^{-1}$) is much smaller than that expected (−84 cm$^{-1}$) for symmetrical bimetallomers.

Hoffman's recent study on symmetrical copper dimers provides a theoretical basis for the dependence of the value of $J$ on the bridge angle. His model is in excellent agreement with the experimental results. Thus, our experimental value of $J$ is quite a bit lower than the value expected from theory for a symmetrical dimer. A slight reduction from the predicted value is certainly expected in our case due to the fact that the earlier correlations deal with symmetrical copper dimers.

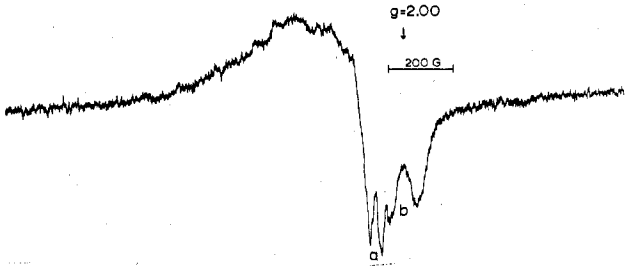


**Figure 3.** Frozen-solution X-band EPR spectrum for Cu(salen)-Cu(hfac)$_2$ at 80 K in 3/2 (v/v) toluene/$CH_2Cl_2$.

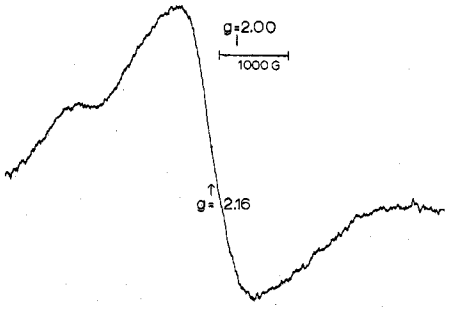


**Figure 4.** X-band EPR powder spectrum for undiluted Cu(salen)-Cu(hfac)$_2$ at 80 K.

However, the large difference observed in the experimental and theoretical value of $J$ indicates that there is something different about the exchange pathway in our copper–copper bimetallomer.

**EPR Investigations.** Relatively little work has been carried out on copper(II) bimetallomers because of complications in attempting to dope them into suitable diamagnetic hosts and because of their insolubility in noncoordinating solvents, in which frozen-solution spectra might be obtained. In the case of the Cu(salen)Cu(hfac)$_2$ bimetallomer, however, there is sufficient solubility in a 3:2 v/v toluene/$CH_2Cl_2$ mixture to investigate the frozen-solution EPR.

The bimetallomer does not exhibit a room-temperature signal as an undiluted powder. When run as a solution at 25 °C (Figure 2), the spectrum observed is the superposition of the isotropic spectra of Cu(salen) and Cu(hfac)$_2$. This is not unexpected as the binuclear complex is about 5% dissociated at $1 \times 10^{-3}$ M concentration on the basis of the equilibrium constant for the bimetallomer formation determined via visible spectroscopic studies.[2] The lack of a signal due to the bimetallomer in the solid state as well as in solution at room temperature is indicative of rapid intramolecular dipolar relaxation. The $^1$H NMR spectrum of the bimetallomer is broad, but observable, and is consistent with the lack of a room-temperature EPR signal.

In an attempt to slow down the relaxation mechanism, the frozen-solution EPR spectrum of the complex was obtained at 80 K. The rather sharp and intense signals at higher fields in Figure 3 are attributed to the presence of monomeric Cu(hfac)$_2$ (a) and Cu(salen) (b). The broad signal at lower fields, which prevents the resolution of the parallel regions of the spectra expected from the monomers, can be assigned to the bimetallomer. This is consistent with the spectrum of the undiluted powder at 80 K (Figure 4) which yields a broad signal with an overall width of approximately 5000 G. The $g$ value of 2.16 obtained from the powder spectrum is similar to that found for other unsymmetrical copper dimers.[3]

In order to try to resolve the broad signal observed for the bimetallomer as a powder, we doped the copper complex into the diamagnetic host Ni(salen)Zn(hfac)$_2$. However, the spectrum of the doped powder at liquid nitrogen temperature is essentially a superposition of the spectra of Cu(salen)Zn-(hfac)$_2$ and Ni(salen)Cu(hfac)$_2$.[18] This indicates that metal

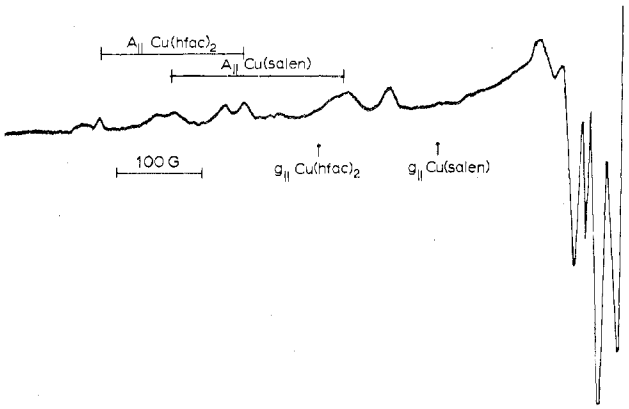


**Figure 5.** The $g_{\parallel}$ region of the X-band EPR spectrum of a frozen toluene/$CH_2Cl_2$ solution of Cu(salen)Cu(hfac)$_2$ at 10 K.

swapping is taking place, presumably in a method similar to that reported for the Cu(salen)Co(hfac)$_2$ bimetallomer.[2] It is evident that doping M(salen)M′(hfac)$_2$ compounds into one another results in undesirable consequences as far as obtaining the EPR spectrum of the copper(II) bimetallomer is concerned. This being the case, liquid helium temperature EPR spectra were obtained with the hope of slowing down the relaxation in an attempt to again examine the bimetallomer signal.

The frozen-solution spectrum of the complex at 10 K (Figure 5) appears complicated, but in fact is not. The $g_{\parallel}$ region shows features due to the two dissociated monomers Cu(salen) and Cu(hfac)$_2$. Each signal is further complicated because several of the hyperfine lines are split into two components due to the different nuclear magnetic moments of the two naturally occurring isotopes $^{63}$Cu and $^{65}$Cu. Not all of the hyperfine components for the parallel region are resolved due to the extensive overlap in the perpendicular region, again attributable to the two monomers. This also prohibits any comparison of $g_{\perp}$ and $A_{\perp}$ values.

For confirmation of the above assignments, especially those in the parallel region, the frozen-solution spectra of Cu(salen) and Cu(hfac)$_2$ were run at 10 K. The outer hyperfine lines in Figure 5 match up with the corresponding copper monomer features, confirming the presence of the two monomers in the frozen solution. The lack of a well-defined EPR signal for the copper bimetallomer at this temperature supports the susceptibility results that indicate that the copper(II) centers are antiferromagnetically coupled.

With the hope that the complex might actually "self-dope" itself, variable-temperature liquid-helium spectra were obtained on the undiluted powder in the range from 50 to 7 K. The only well-resolved spectrum was the one obtained at 7 K, which again indicated signals due to Cu(salen) and Cu(hfac)$_2$ superimposed upon the broad signal attributed to the complex. Computer averaging was used in an attempt to pull information out of the base line and to try to sharpen the features observed. This resulted in no significant increase in resolution over the nonaveraged spectrum obtained.

The EPR spectra of this copper(II) bimetallomer also give results that are atypical of other symmetrical dimers. Symmetrical dimers with exchange parameters of similar magnitude to ours have produced well-resolved EPR spectra.[7] Magnetic-exchange interactions and zero-field effects are observed in these EPR spectra.

In order to better interpret the susceptibility and EPR results, and also to explain the difference in behavior of our compound from those discussed above, we decided that a crystal structure determination would be the only way to provide definite answers to the above experiments.

**X-ray Single-Crystal Investigation.** The crystal structure shows a basic similarity to that of Cu(salen)Co(hfac)$_2$, but some significant differences exist. Cu(salen)Cu(hfac)$_2$ crystallizes in a unit cell containing four molecules in contrast

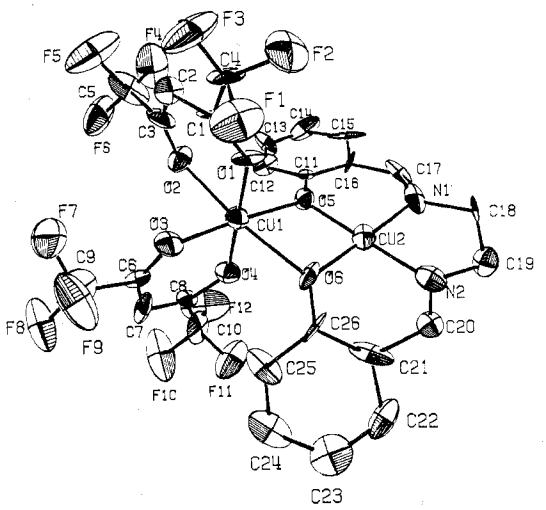


**Figure 6.** ORTEP-II drawing of Cu(salen)Cu(hfac)$_2$ showing the atom numbering for molecule A. The ellipsoids represent 30% probability and hydrogen atoms have been omitted.

**Table I.** Positional Parameters for Molecule A of Cu(salen)Cu(hfac)$_2$

| atom | *x* | *y* | *z* |
|---|---|---|---|
| Cu1 | −0.2718 (2) | −0.5574 (1) | −0.1190 (3) |
| Cu2 | −0.3507 (2) | −0.4301 (2) | −0.0908 (3) |
| O1 | −0.3812 (8) | −0.6236 (8) | −0.2440 (14) |
| O2 | −0.2136 (9) | −0.6076 (8) | −0.2764 (17) |
| O3 | −0.2653 (8) | −0.6423 (7) | −0.0345 (15) |
| O4 | −0.1638 (8) | −0.4918 (7) | 0.0128 (14) |
| O5 | −0.2795 (8) | −0.4647 (6) | −0.1930 (13) |
| O6 | −0.3414 (7) | −0.5015 (7) | 0.0206 (15) |
| N1 | −0.3667 (10) | −0.3624 (8) | −0.2109 (20) |
| N2 | −0.4215 (10) | −0.3919 (10) | 0.0086 (18) |
| C1 | −0.3923 (13) | −0.6812 (10) | −0.3326 (18) |
| C2 | −0.3402 (14) | −0.7074 (13) | −0.4001 (24) |
| C3 | −0.2566 (13) | −0.6654 (12) | −0.3629 (21) |
| C4 | −0.4843 (13) | −0.7282 (12) | −0.3833 (21) |
| C5 | −0.2051 (12) | −0.6853 (16) | −0.4562 (28) |
| C6 | −0.2035 (14) | −0.6426 (9) | 0.0535 (18) |
| C7 | −0.1323 (14) | −0.5894 (12) | 0.1235 (23) |
| C8 | −0.1214 (10) | −0.5211 (10) | 0.0903 (18) |
| C9 | −0.2086 (12) | −0.7194 (15) | 0.0901 (26) |
| C10 | −0.0461 (12) | −0.4531 (13) | 0.1694 (25) |
| C11 | −0.2331 (10) | −0.4268 (10) | −0.2810 (19) |
| C12 | −0.1672 (13) | −0.4454 (11) | −0.3151 (22) |
| C13 | −0.1223 (13) | −0.4145 (12) | −0.4037 (25) |
| C14 | −0.1374 (20) | −0.3577 (18) | −0.4680 (28) |
| C15 | −0.2048 (13) | −0.3356 (10) | −0.4383 (19) |
| C16 | −0.2519 (13) | −0.3692 (13) | −0.3340 (25) |
| C17 | −0.3139 (9) | −0.3396 (8) | −0.3016 (19) |
| C18 | −0.4328 (11) | −0.3279 (10) | −0.1842 (20) |
| C19 | −0.4489 (12) | −0.3318 (11) | −0.0436 (24) |
| C20 | −0.4428 (10) | −0.4159 (9) | 0.1200 (18) |
| C21 | −0.4082 (14) | −0.4689 (12) | 0.1937 (21) |
| C22 | −0.4314 (15) | −0.4721 (14) | 0.3296 (37) |
| C23 | −0.3970 (21) | −0.5109 (15) | 0.4115 (35) |
| C24 | −0.3476 (15) | −0.5501 (16) | 0.3712 (33) |
| C25 | −0.3280 (12) | −0.5479 (13) | 0.2388 (30) |
| C26 | −0.3621 (10) | −0.5081 (10) | 0.1426 (21) |
| F1 | −0.5224 (9) | −0.7374 (9) | −0.2703 (18) |
| F2 | −0.5310 (10) | −0.6898 (9) | −0.4429 (20) |
| F3 | −0.5051 (9) | −0.7877 (9) | −0.4594 (20) |
| F4 | −0.1850 (14) | −0.6459 (11) | −0.5475 (20) |
| F5 | −0.2362 (10) | −0.7568 (11) | −0.5220 (22) |
| F6 | −0.1276 (10) | −0.6820 (9) | −0.3976 (19) |
| F7 | −0.2174 (17) | −0.7658 (11) | −0.0256 (23) |
| F8 | −0.1477 (10) | −0.7258 (8) | 0.1793 (21) |
| F9 | −0.2775 (11) | −0.7523 (11) | 0.1194 (24) |
| F10 | 0.0083 (9) | −0.4730 (8) | 0.2538 (22) |
| F11 | −0.0620 (9) | −0.4062 (9) | 0.2530 (19) |
| F12 | 0.0014 (10) | −0.4127 (11) | 0.1047 (19) |

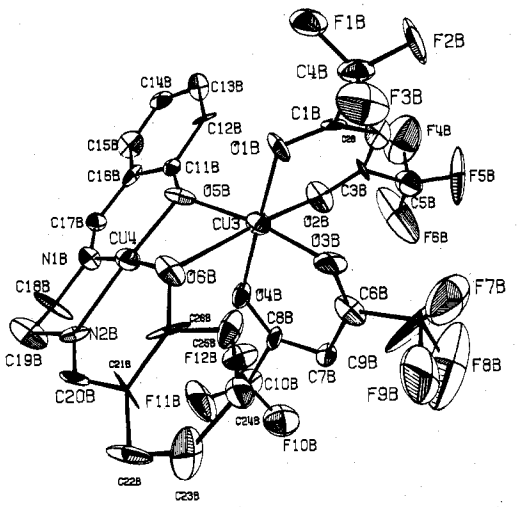


**Figure 7.** ORTEP-II drawing of Cu(salen)Cu(hfac)$_2$ showing the atom numbering for molecule B. The ellipsoids represent 30% probability and hydrogen atoms have been omitted.

**Table II.** Bond Lengths (Å) for Molecule A of Cu(salen)Cu(hfac)$_2$

| | | | |
|---|---|---|---|
| Cu1-Cu2 | 3.124 (4) | C9-F7 | 1.321 (37) |
| Cu1-O1 | 2.000 (12) | C9-F8 | 1.284 (34) |
| Cu1-O2 | 2.260 (15) | C9-F9 | 1.252 (35) |
| Cu1-O3 | 1.932 (14) | C8-C10 | 1.532 (24) |
| Cu1-O4 | 2.009 (13) | C10-F10 | 1.309 (29) |
| Cu1-O5 | 2.024 (11) | C10-F11 | 1.272 (30) |
| Cu1-O6 | 2.335 (12) | C10-F12 | 1.255 (34) |
| Cu2-O5 | 1.923 (12) | O5-C11 | 1.394 (21) |
| Cu2-O6 | 1.876 (14) | C11-C12 | 1.358 (23) |
| Cu2-N1 | 1.899 (18) | C12-C13 | 1.335 (23) |
| Cu2-N2 | 1.934 (17) | C13-C14 | 1.384 (31) |
| O1-C1 | 1.269 (22) | C14-C15 | 1.402 (31) |
| C1-C2 | 1.373 (26) | C15-C16 | 1.499 (27) |
| C2-C3 | 1.364 (26) | C11-C16 | 1.371 (24) |
| O2-C3 | 1.249 (24) | C16-C17 | 1.407 (25) |
| C1-C4 | 1.509 (23) | C17-N1 | 1.392 (23) |
| C4-F1 | 1.389 (28) | N1-C18 | 1.513 (21) |
| C4-F2 | 1.344 (30) | C18-C19 | 1.471 (25) |
| C4-F3 | 1.205 (28) | C19-N2 | 1.476 (22) |
| C3-C5 | 1.474 (27) | N2-C20 | 1.308 (22) |
| C5-F4 | 1.268 (32) | C20-C21 | 1.512 (27) |
| C5-F5 | 1.344 (35) | C21-C22 | 1.469 (30) |
| C5-F6 | 1.324 (25) | C22-C23 | 1.335 (33) |
| O3-C6 | 1.244 (25) | C23-C24 | 1.366 (33) |
| C6-C7 | 1.332 (27) | C24-C25 | 1.410 (29) |
| C7-C8 | 1.348 (23) | C25-C26 | 1.435 (28) |
| O4-C8 | 1.256 (20) | C26-C21 | 1.358 (26) |
| C6-C9 | 1.533 (26) | C26-O6 | 1.325 (24) |

to the two molecules per unit cell for the Cu–Co bimetallomer. Thus, the asymmetric unit for the Cu–Cu system contains two molecules, which we shall label as molecule A and molecule B (Figures 6 and 7). Positional parameters, bond lengths, and bond angles for the two molecules are given in Tables I–VI. Thermal parameters and root-mean-square amplitudes of vibration are listed in Tables VII–X and are available as supplementary material. The two molecules, A and B, have different bond lengths and bond angles around the bridge area and as a result are not enantiomeric pairs.[20] Thus, each unit cell consists of two pairs of enantiomers: A and its inverse as well as B and its inverse. The fact that the two molecules, A and B, are different supports the observation of the unit cell having four molecules.

As in the Cu–Co case, the Cu(salen) fragment contains the copper atom in a square-planar environment. The copper atom in the hfac environment is again six-coordinate, but the change from cobalt to copper has produced a dramatic distortion of the six-coordinate environment about the metal center. In the case of both molecule A and molecule B, a tetragonal elongation exists along the $d_{z^2}$ axis. The $d_{z^2}$ orbital in molecule

**Table III.** Bond Angles (deg) for Molecule A of Cu(salen)Cu(hfac)$_2$

| | | | |
|---|---|---|---|
| O1-Cu1-O2 | 83.9 (5) | C3-C5-F4 | 119.6 (25) |
| O1-Cu1-O3 | 88.2 (6) | C3-C5-F5 | 113.9 (21) |
| O1-Cu1-O4 | 177.9 (6) | C3-C5-F6 | 117.1 (24) |
| O1-Cu1-O5 | 93.7 (6) | F4-C5-F5 | 106.6 (28) |
| O1-Cu1-O6 | 92.0 (5) | F4-C5-F6 | 96.9 (22) |
| O2-Cu1-O3 | 82.4 (6) | F5-C5-F6 | 99.8 (28) |
| O2-Cu1-O4 | 97.7 (5) | O3-C6-C7 | 133.2 (20) |
| O2-Cu1-O5 | 101.7 (5) | O3-C6-C9 | 114.6 (20) |
| O2-Cu1-O6 | 173.0 (5) | C7-C6-C9 | 112.2 (22) |
| O3-Cu1-O4 | 90.7 (5) | C6-C7-C8 | 115.3 (22) |
| O3-Cu1-O5 | 175.6 (6) | O4-C8-C7 | 136.3 (21) |
| O3-Cu1-O6 | 103.2 (5) | O4-C8-C10 | 101.9 (18) |
| O4-Cu1-O5 | 87.3 (5) | C7-C8-C10 | 121.4 (19) |
| O4-Cu1-O6 | 86.6 (5) | C6-C9-F7 | 108.6 (25) |
| O5-Cu1-O6 | 72.8 (5) | C6-C9-F8 | 119.4 (23) |
| O5-Cu2-O6 | 86.2 (5) | C6-C9-F9 | 112.8 (21) |
| O5-Cu2-N1 | 93.9 (7) | F7-C9-F8 | 106.4 (31) |
| N1-Cu2-O6 | 176.3 (6) | F7-C9-F9 | 97.8 (31) |
| N1-Cu2-N2 | 84.0 (8) | F8-C9-F9 | 109.3 (40) |
| N2-Cu2-O5 | 177.8 (7) | C8-C10-F10 | 111.2 (20) |
| O6-Cu2-N2 | 95.9 (7) | C8-C10-F11 | 116.6 (17) |
| Cu1-O1-C1 | 126.8 (15) | C8-C10-F12 | 120.6 (23) |
| Cu1-O2-C3 | 120.7 (15) | F10-C10-F11 | 101.4 (32) |
| Cu1-O3-C6 | 124.6 (14) | F10-C10-F12 | 101.2 (26) |
| Cu1-O4-C8 | 119.1 (14) | F11-C10-F12 | 103.3 (30) |
| Cu1-O5-Cu2 | 104.7 (6) | O5-C11-C12 | 120.9 (22) |
| Cu1-O5-C11 | 128.0 (13) | O5-C11-C16 | 121.0 (23) |
| Cu2-O5-C11 | 126.5 (13) | C12-C11-C16 | 118.1 (21) |
| Cu1-O6-C26 | 136.1 (15) | C11-C12-C13 | 124.6 (22) |
| Cu1-O6-Cu2 | 95.2 (6) | C12-C13-C14 | 122.5 (24) |
| Cu2-O6-C26 | 128.4 (14) | C13-C14-C15 | 116.2 (25) |
| Cu2-N1-C17 | 122.1 (13) | C14-C15-C16 | 120.0 (25) |
| Cu2-N1-C18 | 114.0 (15) | C15-C16-C17 | 116.5 (26) |
| C17-N1-C18 | 123.2 (19) | C11-C16-C15 | 118.1 (20) |
| Cu2-N2-C19 | 117.1 (14) | C11-C16-C17 | 125.3 (26) |
| Cu2-N2-C20 | 122.3 (15) | N1-C17-C16 | 127.0 (20) |
| C19-N2-C20 | 120.6 (19) | N1-C18-C19 | 112.2 (17) |
| O1-C1-C2 | 134.3 (23) | N2-C19-C18 | 108.5 (18) |
| O1-C1-C4 | 122.6 (20) | N2-C20-C21 | 124.8 (22) |
| C2-C1-C4 | 112.8 (18) | C20-C21-C22 | 110.4 (30) |
| C1-C2-C3 | 115.5 (22) | C20-C21-C26 | 125.2 (26) |
| O2-C3-C2 | 134.9 (24) | C22-C21-C26 | 124.5 (25) |
| O2-C3-C5 | 110.2 (21) | C21-C22-C23 | 116.1 (28) |
| C2-C3-C5 | 114.3 (21) | C22-C23-C24 | 123.5 (35) |
| C1-C4-F1 | 109.7 (18) | C23-C24-C25 | 119.3 (30) |
| C1-C4-F2 | 112.1 (22) | C24-C25-C26 | 121.5 (25) |
| C1-C4-F3 | 120.9 (21) | O6-C26-C21 | 121.7 (27) |
| F1-C4-F2 | 95.9 (24) | O6-C26-C25 | 123.0 (24) |
| F1-C4-F3 | 108.8 (31) | C21-C26-C25 | 114.7 (25) |
| F2-C4-F3 | 106.6 (25) | | |

A is apparently directed toward oxygen atoms O6 and O2 on the basis of the six copper–oxygen distances. The lengthening of the Cu1–O2 bond by more than 0.2 Å and the Cu1–O6 bond by more than 0.3 Å over the other four copper–oxygen bonds clearly defines the general location of the $d_{z^2}$ orbital. The $d_{x^2-y^2}$ orbital for Cu1 would then have its lobes directed at oxygen atoms O1, O3, O4, and O5. The corresponding $d_{x^2-y^2}$ orbital of Cu2 would be directed toward nitrogen atoms N1 and N2 and oxygen atoms O5 and O6.

In looking at molecule B, we see the $d_{z^2}$ orbital for copper atom Cu3 has its lobes directed at oxygen atoms O6B and O2B with the $d_{x^2-y^2}$ orbital being directed at oxygen atoms O1B, O3B, O4B, and O5B. It is interesting to note that the Cu3–O6B bond length of 2.576 (12) Å is quite a bit longer than the other copper–oxygen distances in the asymmetric unit and, indeed, longer than the Cu3–O2B length of 2.305 (11) Å. The difference Fourier map shows that atom O6B is correctly placed, which indicates that in molecule B either the $d_{z^2}$ orbital contains a sizable amount of other orbital character or else its "lengthening" toward O6B is due to crystal packing and the attempt to minimize steric repulsions. The $d_{x^2-y^2}$ orbital of atom Cu4 has its lobes directed toward nitrogen atoms N1B and N2B and oxygen atoms O5B and O6B.

**Table IV.** Positional Parameters for Molecule B of Cu(salen)Cu(hfac)$_2$

| atom | $x$ | $y$ | $z$ |
|---|---|---|---|
| Cu3 | −0.2341 (2) | −0.0588 (1) | −0.0758 (3) |
| Cu4 | −0.0719 (2) | −0.0790 (1) | −0.1233 (3) |
| O1B | −0.2339 (8) | −0.0165 (7) | 0.1103 (14) |
| O2B | −0.3679 (7) | −0.1389 (6) | −0.0848 (13) |
| O3B | −0.2888 (10) | 0.0124 (9) | −0.1440 (15) |
| O4B | −0.2371 (8) | −0.1001 (7) | −0.2692 (14) |
| O5B | −0.1557 (8) | −0.1150 (8) | −0.0161 (12) |
| O6B | −0.0853 (7) | 0.0183 (7) | −0.0977 (13) |
| N1B | −0.0540 (10) | −0.1730 (10) | −0.1667 (19) |
| N2B | 0.0077 (8) | −0.0459 (8) | −0.2473 (13) |
| C1B | −0.2998 (9) | −0.0096 (9) | 0.1456 (16) |
| C2B | −0.3891 (15) | −0.0526 (11) | 0.0916 (23) |
| C3B | −0.4095 (11) | −0.1083 (10) | −0.0177 (19) |
| C4B | −0.2829 (13) | 0.0531 (11) | 0.2726 (19) |
| C5B | −0.5065 (11) | −0.1454 (9) | −0.0913 (18) |
| C6B | −0.3213 (11) | 0.0071 (10) | −0.2613 (19) |
| C7B | −0.3189 (12) | −0.0331 (11) | −0.3912 (20) |
| C8B | −0.2763 (10) | −0.0835 (11) | −0.3750 (20) |
| C9B | −0.3829 (30) | 0.0512 (18) | −0.2737 (27) |
| C10B | −0.2624 (14) | −0.1229 (11) | −0.5156 (22) |
| C11B | −0.1731 (11) | −0.1808 (13) | 0.0242 (21) |
| C12B | −0.2247 (12) | −0.1925 (10) | 0.1293 (18) |
| C13B | −0.2449 (11) | −0.2566 (10) | −0.1907 (21) |
| C14B | −0.2129 (13) | −0.3148 (11) | 0.1504 (20) |
| C15B | −0.1612 (13) | −0.3044 (12) | 0.0456 (25) |
| C16B | −0.1377 (11) | −0.2354 (9) | −0.0074 (18) |
| C17B | −0.0825 (10) | −0.0230 (09) | −0.1112 (18) |
| C18B | −0.0061 (14) | −0.1813 (11) | −0.2774 (23) |
| C19B | 0.0484 (13) | −0.1054 (13) | −0.2754 (22) |
| C20B | 0.0265 (15) | 0.0168 (17) | −0.2912 (24) |
| C21B | −0.0120 (11) | 0.0776 (14) | −0.2776 (21) |
| C22B | 0.0092 (15) | 0.1423 (17) | −0.3411 (24) |
| C23B | −0.0302 (17) | 0.1898 (12) | −0.3061 (31) |
| C24B | −0.0850 (14) | 0.1861 (13) | −0.2183 (26) |
| C25B | −0.1022 (12) | 0.1304 (15) | −0.1483 (23) |
| C26B | −0.0600 (12) | 0.0740 (10) | −0.1774 (19) |
| F1B | −0.2275 (8) | 0.0465 (7) | 0.3780 (13) |
| F2B | −0.3508 (8) | 0.0555 (8) | 0.3160 (14) |
| F3B | −0.2491 (10) | 0.1160 (8) | 0.2297 (16) |
| F4B | −0.5312 (10) | −0.1965 (13) | −0.0032 (25) |
| F5B | −0.5517 (7) | −0.1090 (8) | −0.0700 (19) |
| F6B | −0.5247 (9) | −0.1903 (17) | −0.1959 (22) |
| F7B | −0.3787 (39) | 0.0969 (33) | −0.1971 (25) |
| F8B | −0.4269 (21) | 0.0451 (23) | −0.3908 (74) |
| F9B | −0.3406 (37) | 0.1090 (26) | −0.3327 (71) |
| F10B | −0.3108 (9) | −0.1170 (8) | −0.6208 (15) |
| F11B | −0.1880 (9) | −0.1080 (10) | −0.5196 (14) |
| F12B | −0.2916 (8) | −0.1991 (7) | −0.5135 (12) |

**Table V.** Bond Lengths (Å) for Molecule B of Cu(salen)Cu(hfac)$_2$

| | | | |
|---|---|---|---|
| Cu3–Cu4 | 3.011 (3) | C9B–F7B | 1.066 (47) |
| Cu3–O1B | 1.923 (13) | C9B–F8B | 1.237 (50) |
| Cu3–O2B | 2.305 (11) | C9B–F9B | 1.375 (132) |
| Cu3–O3B | 1.983 (16) | C8B–C10B | 1.595 (24) |
| Cu3–O4B | 1.971 (13) | C10B–F10B | 1.249 (25) |
| Cu3–O5B | 2.007 (13) | C10B–F11B | 1.219 (31) |
| Cu3–O6B | 2.576 (12) | C10B–F12B | 1.392 (29) |
| Cu4–O5B | 1.933 (12) | O5B–C11B | 1.326 (20) |
| Cu4–O6B | 1.935 (13) | C11B–C12B | 1.468 (22) |
| Cu4–N1B | 1.923 (16) | C12B–C13B | 1.407 (21) |
| Cu4–N2B | 1.996 (17) | C13B–C14B | 1.426 (22) |
| O1B–C1B | 1.271 (18) | C14B–C15B | 1.466 (24) |
| C1B–C2B | 1.458 (23) | C15B–C16B | 1.443 (24) |
| C2B–C3B | 1.342 (22) | C11B–C16B | 1.387 (23) |
| O2B–C3B | 1.269 (18) | C16B–C17B | 1.501 (21) |
| C1B–C4B | 1.554 (22) | C17B–N1B | 1.277 (20) |
| C4B–F1B | 1.324 (23) | N1B–C18B | 1.498 (22) |
| C4B–F2B | 1.312 (26) | C18B–C19B | 1.461 (23) |
| C4B–F3B | 1.319 (26) | C19B–N2B | 1.525 (23) |
| C3B–C5B | 1.584 (21) | N2B–C20B | 1.288 (23) |
| C5B–F4B | 1.403 (25) | C20B–C21B | 1.503 (34) |
| C5B–F5B | 1.212 (22) | C21B–C22B | 1.427 (33) |
| C5B–F6B | 1.194 (24) | C22B–C23B | 1.332 (30) |
| O3B–C6B | 1.174 (23) | C23B–C24B | 1.374 (28) |
| C6B–C7B | 1.432 (26) | C24B–C25B | 1.321 (24) |
| C7B–C8B | 1.379 (23) | C25B–C26B | 1.496 (28) |
| O4B–C8B | 1.265 (20) | C26B–C21B | 1.386 (22) |
| C6B–C9B | 1.530 (30) | C26B–O6B | 1.405 (19) |

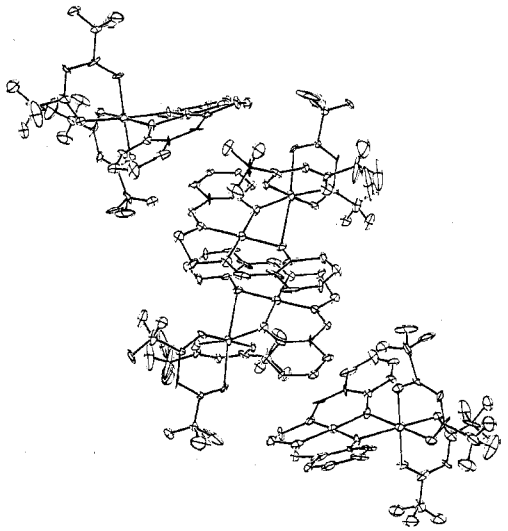

**Figure 8.** Perspective view showing the packing of Cu(salen)Cu(hfac)$_2$ molecules in the crystal.

Another aspect of the structure worth noting is the copper–copper distance in molecule A and molecule B. Both distances seem to preclude any significant metal–metal bond. The shortened Cu3–Cu4 distance is due to the different geometry of molecule B relative to molecule A. The salen and hfac portions are tipped more toward each other than in molecule A, and this is reflected in the dihedral angle between planes intersecting at the bridging phenolic oxygen atoms. The angle between plane 2 (atoms O5, O6, N1, N2, Cu2) and plane 5 (atoms O2, O3, O5, O6, Cu1) is 167.8°. This can be compared to the angle between plane 7 (atoms N1B, N2B, O5B, O6B, Cu4) and plane 10 (atoms O5B, O6B, Cu3, O2B, O3B) of 135.4°. The difference in angles here is probably a result of crystal packing and the orientations of the two molecules in the unit cell (Figure 8). The angle between planes 2 and 5 is also comparable to that observed in the Cu–Co structure.

The salen moiety for both molecules A and B has a convex shape, as was the case for the Cu–Co bimetallomer. The angle between plane 3 (C21, C22, C23, C24, C25, C26) and plane 4 (C11, C12, C13, C14, C15, C16) is 152.6°, which indicates not as much bending between the phenyl rings as observed in the Cu–Co structure. Even less bending is seen between the phenyl rings for molecule B. The angle between plane 8 (C11B, C12B, C13B, C14B, C15B, C16B) and plane 9 (C21B, C22B, C23B, C24B, C25B, C26B) is 175.1°, which gives an almost planar salen fragment. The packing in the unit cell can be seen to minimize steric repulsions in adjacent salen rings by having the molecules alternately oriented with their phenyl rings up and then down.

The most important feature of the structure is the bridge area, because it enables the magnetic susceptibility results to be interpreted. One of the copper(II) centers has an unpaired electron that occupies the $d_{x^2-y^2}$ orbital in the square-planar salen portion of the bimetallomer. The other copper(II) (surrounded by six oxygen atoms), being in a tetragonally elongated geometry, also has its unpaired electron occupying a $d_{x^2-y^2}$ orbital. However, owing to the orientation of the $d_{x^2-y^2}$ orbital of the six-coordinate copper atom, only one phenolic oxygen is common to each $d_{x^2-y^2}$ plane. Thus, the pathway for superexchange between copper centers does not include both bridging phenolic oxygens. The angle between the $d_{x^2-y^2}$ orbitals can give an approximate indication of the type of p

**Table VI.** Bond Angles (deg) for Molecule B of $Cu(salen)Cu(hfac)_2$

| | | | |
|---|---|---|---|
| O1B-Cu3-O2B | 87.2 (5) | C3B-C5B-F4B | 99.3 (17) |
| O1B-Cu3-O3B | 87.6 (6) | C3B-C5B-F5B | 116.2 (19) |
| O1B-Cu3-O4B | 177.9 (6) | C3B-C5B-F6B | 117.8 (19) |
| O1B-Cu3-O5B | 95.4 (5) | F4B-C5B-F5B | 97.6 (19) |
| O1B-Cu3-O6B | 100.8 (5) | F4B-C5B-F6B | 96.7 (22) |
| O2B-Cu3-O3B | 87.3 (6) | F5B-C5B-F6B | 120.6 (24) |
| O2B-Cu3-O4B | 92.3 (5) | O3B-C6B-C7B | 134.9 (25) |
| O2B-Cu3-O5B | 105.3 (5) | O3B-C6B-C9B | 110.6 (19) |
| O2B-Cu3-O6B | 171.8 (4) | C7B-C6B-C9B | 114.5 (20) |
| O3B-Cu3-O4B | 90.3 (5) | C6B-C7B-C8B | 113.2 (19) |
| O3B-Cu3-O5B | 167.1 (6) | O4B-C8B-C7B | 133.1 (22) |
| O3B-Cu3-O6B | 94.8 (5) | O4B-C8B-C10B | 111.0 (16) |
| O4B-Cu3-O5B | 86.7 (5) | C7B-C8B-C10B | 115.3 (17) |
| O4B-Cu3-O6B | 79.7 (4) | C6B-C9B-F7B | 123.9 (39) |
| O5B-Cu3-O6B | 72.4 (5) | C6B-C9B-F8B | 117.3 (29) |
| O5B-Cu4-O6B | 90.4 (6) | C6B-C9B-F9B | 100.8 (41) |
| O5B-Cu4-N1B | 95.4 (7) | F7B-C9B-F8B | 116.6 (49) |
| N1B-Cu4-O6B | 173.7 (7) | F7B-C9B-F9B | 80.8 (92) |
| N1B-Cu4-N2B | 83.6 (8) | F8B-C9B-F9B | 73.1 (54) |
| N2B-Cu4-O5B | 175.5 (6) | C8B-C10B-F10B | 111.8 (17) |
| O6B-Cu4-N2B | 90.4 (7) | C8B-C10B-F11B | 113.0 (20) |
| Cu3-O1B-C1B | 122.8 (12) | C8B-C10B-F12B | 105.4 (18) |
| Cu3-O2B-C3B | 112.3 (11) | F10B-C10B-F11B | 116.6 (28) |
| Cu3-O3B-C6B | 123.3 (17) | F10B-C10B-F12B | 102.9 (26) |
| Cu3-O4B-C8B | 123.4 (13) | F11B-C10B-F12B | 105.6 (20) |
| Cu3-O5B-Cu4 | 99.7 (6) | O5B-C11B-C12B | 116.7 (19) |
| Cu3-O5B-C11B | 129.0 (12) | O5B-C11B-C16B | 126.3 (20) |
| Cu4-O5B-C11B | 124.2 (13) | C12B-C11B-C16B | 116.3 (20) |
| Cu3-O6B-C26B | 130.3 (14) | C11B-C12B-C13B | 124.7 (18) |
| Cu3-O6B-Cu4 | 82.4 (4) | C12B-C13B-C14B | 118.4 (18) |
| Cu4-O6B-C26B | 126.0 (16) | C13B-C14B-C15B | 117.8 (18) |
| Cu4-N1B-C17B | 124.8 (15) | C14B-C15B-C16B | 121.4 (20) |
| Cu4-N1B-C18B | 118.0 (13) | C15B-C16B-C17B | 117.0 (19) |
| C17B-N1B-C18B | 117.2 (18) | C11B-C16B-C15B | 120.7 (22) |
| Cu4-N2B-C19B | 108.6 (14) | C11B-C16B-C17B | 121.9 (21) |
| Cu4-N2B-C20B | 126.9 (18) | N1B-C17B-C16B | 125.7 (20) |
| C19B-N2B-C20B | 124.4 (22) | N1B-C18B-C19B | 104.5 (17) |
| O1B-C1B-C2B | 131.2 (18) | N2B-C19B-C18B | 113.9 (19) |
| O1B-C1B-C4B | 115.0 (15) | N2B-C20B-C21B | 129.5 (26) |
| C2B-C1B-C4B | 113.8 (16) | C20B-C21B-C22B | 124.6 (26) |
| C1B-C2B-C3B | 117.8 (19) | C20B-C21B-C26B | 114.6 (34) |
| O2B-C3B-C2B | 134.8 (20) | C22B-C21B-C26B | 119.9 (30) |
| O2B-C3B-C5B | 107.9 (16) | C21B-C22B-C23B | 112.7 (26) |
| C2B-C3B-C5B | 117.2 (17) | C22B-C23B-C24B | 130.0 (27) |
| C1B-C4B-F1B | 110.2 (16) | C23B-C24B-C25B | 120.2 (22) |
| C1B-C4B-F2B | 114.5 (18) | C24B-C25B-C26B | 114.5 (21) |
| C1B-C4B-F3B | 105.2 (16) | O6B-C26B-C21B | 129.9 (33) |
| F1B-C4B-F2B | 108.9 (20) | O6B-C26B-C25B | 107.8 (26) |
| F1B-C4B-F3B | 108.7 (28) | C21B-C26B-C25B | 122.0 (24) |
| F2B-C4B-F3B | 109.0 (21) | | |

or p-type hybrid orbital on the oxygen which allows for superexchange. The angle between plane 1 (O1, O2, Cu1, O4, O5) and plane 2 (O5, O6, N1, N2, Cu2) is 93.0°. Molecule B appears to give slightly different information in that the angle between plane 6 (O1B, O3B, O4B, O5B, Cu3) and plane 7 (N1B, N2B, O5B, O6B, Cu4) is 120.0°. This difference is also reflected in the corresponding bond angles Cu2–O5–Cu1, 104.7 (6)°, and Cu3–O5B–Cu4, 99.7 (6)°. With the decrease in the bond angle in molecule B, the dihedral angle between planes 6 and 7 opens up. The bridge angle in both cases is between that expected for orthogonal p orbitals (90°) and $sp^3$ hybridization (109.5°). This is more or less expected due to the remaining lone pair of electrons on the phenolic oxygen. While there is undoubtedly substantial orbital mixing in the bridge area, it seems reasonable to attribute the reduced value of $J$, therefore, to the relative orientation of metal orbitals on the two copper centers containing the unpaired electrons. The reduced symmetry of the bridge area provides only one phenolic oxygen connecting the essentially metal orbitals containing the unpaired electrons for a superexchange pathway. It is also evident that the previously mentioned correlations using doubly bridged dimers cannot be extended (even roughly) to such a distorted and unsymmetrical system.

**Acknowledgment.** We are grateful to the National Science Foundation for support through Grants CHE 76-20664 (R.S.D.) and CHE 77-24964 (G.D.S.). We are also grateful to Professor David N. Hendrickson and Dr. Ed Laskowski for collecting the low-temperature magnetic susceptibility data and providing helpful discussions concerning its interpretation. Mr. William Willis deserves a special thanks for his expert assistance during the structure determination.

**Registry No.** $Cu(salen)Cu(hfac)_2$, 62303-69-9; $Ni(salen)Zn(hfac)_2$, 69942-20-7; Ni(salen), 14167-20-5; $Zn(hfac)_2$, 14949-70-3.

**Supplementary Material Available:** Tables VII–X containing thermal parameters and root-mean-square amplitudes of vibration, Table XI containing observed and theoretically calculated variable-temperature magnetic susceptibility data, and Table XII listing observed and calculated structure factor amplitudes (38 pages). Ordering information is given on any current masthead page.

## References and Notes


(1) N. B. O'Bryan, T. O. Maier, I. C. Paul, and R. S. Drago, *J. Am. Chem. Soc.*, **95**, 6640 (1973).
(2) D. J. Kitko, K. E. Wiegers, S. G. Smith, and R. S. Drago, *J. Am. Chem. Soc.*, **99**, 1410 (1977).
(3) E. Sinn and C. M. Harris, *Coord. Chem. Rev.*, **4**, 391 (1969).
(4) R. M. Countryman, W. T. Robinson, and E. Sinn, *Inorg. Chem.*, **13**, 2013 (1974).
(5) P. J. Hay, J. C. Thibeault, and R. Hoffmann, *J. Am. Chem. Soc.*, **97**, 4884 (1975).
(6) V. H. Crawford, H. W. Richardson, J. R. Wasson, D. J. Hodgson, and W. E. Hatfield, *Inorg. Chem.*, **15**, 2107 (1976).
(7) E. F. Hasty, T. J. Colburn, and D. N. Hendrickson, *Inorg. Chem.*, **12**, 2414 (1973).
(8) W. L. Jolly, "The Synthesis and Characterization of Inorganic Compounds", Prentice-Hall, Englewood Cliffs, NJ, 1970, p 371.
(9) J. P. Chandler, Program 66, Quantum Chemistry Program Exchange, Indiana University, Bloomington, IN, 1973.
(10) Varian Associates standard sample, No. 904450-01.
(11) Stephen L. Lawton and Robert A. Jacobson, "The Reduced Cell and Its Crystallographic Applications", USAEC Report, Ames Laboratory at Iowa State University, Ames, Iowa, 1965.
(12) P. G. Lenhert, *J. Appl. Crystallogr.*, **8**, 568 (1975).
(13) Local version of ORABS: D. J. Wehe, W. R. Busing, and H. A. Levy, USAEC Report ORNL-TM-229, Oak Ridge National Laboratory, Oak Ridge, TN, 1962.
(14) E. R. Howells, D. C. Phillips, and D. Rogers, *Acta Crystallogr.*, **3**, 210 (1950).
(15) Programs used: JIMDAP, the general-plane Fourier mapping program modified by J. Ibers and F. Ross from the original version FORDAP by H. Zalkin and D. H. Templeton; ORXFLS3, the least-squares program based on ORFLS by W. R. Busing, K. O. Martin, and H. A. Levy with modifications by R. D. Ellison, W. C. Hamilton, J. A. Ibers, C. K. Johnson, and W. E. Thiessen; ORFFE3, the crystallographic function and error program based on ORFFE by W. R. Busing, K. O. Martin, and H. A. Levy with modifications by G. M. Brown, C. K. Johnson, and W. F. Thiessen; ORTEPII, the thermal-ellipsoid plot program by C. K. Johnson; MEAN PLANE, a program to calculate angles between planes and deviation from planes by M. E. Pippy and F. R. Ahmed.
(16) D. T. Cromer and J. T. Waber, "International Tables for X-Ray Crystallography", Vol. IV, Kynoch Press, Birmingham, England, 1974, Table 2.
(17) D. T. Cromer and D. Liberman, *J. Chem. Phys.*, **53**, 1891 (1970).
(18) D. J. Kitko, Ph.D. Thesis, University of Illinois, 1976.
(19) D. R. McMillin, R. S. Drago, and J. Nusz, *J. Am. Chem. Soc.*, **98**, 3120 (1976).
(20) Dr. Roger Cramer has suggested that the differences in the bond lengths and bond angles of molecule A and molecule B might be an artifact of the refinement procedure as reported[21] for a structure that refined to a false minimum. In this case, we feel that the structural differences and values of $R$ and $R_w$ can be explained in terms of crystal packing and thermal motion. The values of $R$ and $R_w$ are consistent with those obtained for $Cu(salen)Co(hfac)_2$, since $Cu(salen)Cu(hfac)_2$ crystallizes with four molecules per unit cell, as compared with two molecules per unit cell for $Cu(salen)Co(hfac)_2$. The extra $CF_3$ groups present in this study have increased the amount of thermal motion present in the unit cell by a factor of 2, so the agreement indices will naturally reflect this added motion and disorder. We have repositioned atoms throughout the refinement procedure and feel confident that the structure has been solved with the exception of the $CF_3$ disorder. The geometric differences in the two molecules are reasonable when one considers that tetragonal copper(II) systems show a wide range of axial bond lengths. Thus, slight packing differences could very easily geometrically distort an axial bond length.
(21) F. A. Cotton and G. W. Rice, *Inorg. Chem.*, **17**, 688 (1978).